Research on a terahertz metamaterial biosensor with integrated microfluidic

JIANJUN LIU*
School of Intelligent Engineering, Shaoguan University, Shaoguan Guangdong 512005, China

A terahertz metamaterial biosensor with integrated microfluidic is proposed in this paper. The sensor integrates a microfluidic between the traditional metal resonant structure and the metal base plate, which can produce a perfect absorption peak at 0.827 THz, and the refractive index sensitivity is 225.1GHz/RIU. The research results of this paper show that the existence of microfluidic significantly expands the overlap of electromagnetic wave and analyte and enhances the coupling reaction, which can not only realize the direct detection of liquid samples, but also greatly improve the sensitivity of the sensor.

(Received March 23, 2023; accepted February 12, 2024)

Keywords: Microfluidic, Terahertz, Sensor, Absorption peak

1. Introduction

The early work is to use metamaterials as sensors to realize the sensing detection of biological proteins [1-4] and antibiotics [5-6] which are attached to the surface of metamaterials after drying. However, because the solution environment of the dried samples is very different from that of the actual organisms, and most biological samples can maintain their biological activity only in the liquid environment, the dried samples cannot accurately characterize the information of biological samples. Because of the strong absorption of water in the THz domain, in order to maintain the solution environment of the organism, reducing the thickness of the solution is an effective way to reduce the terahertz wave absorption of water. Researchers put metamaterials in solution cavities to explore their applications in drug reaction monitoring [7] and mixture detection [8], but quantitative detection is still very difficult. The microfluidic chip technology developed in recent years provides a new way to fabricate terahertz biosensors [9-11]. Microfluidic chip technology can accurately control the microfluidic at the micron level, which is an ideal choice for the fabrication of terahertz biosensors. In recent years, microfluidic chips have been used in the sensing detection of isopropanol-water and acetonitrile-water mixtures in terahertz band [12] and the detection of specific virus samples [13]. However, using the microchannel as the sensor, the measurement results are not intuitive enough, which increases the difficulty for the analysis of the results. Therefore, by combining the metamaterial with specific resonance response with the microfluidic chip, the change of liquid characteristics in the microchannel can be easily observed by observing the movement of the metamaterial formant in the frequency spectrum. In 2016, several research groups at home and abroad tried to integrate metamaterials into microfluidic chips for the detection of different organic solutions [14] and glucose solutions [15-16]. Recently, part of the work has also shown its development potential in liver cancer diagnosis [17] and biosensor [18-21].

To sum up, based on the metamaterial absorber, a high sensitivity terahertz microfluidic biosensor based on metamaterial absorber is designed by combining microfluidic technology. The sensor can produce a perfect absorption peak with an absorptivity of 99.83% in the 0.2-1.5THz band, its sensitivity can reach 225.1GHz/RIU, Q value can reach 32.8, and high FOM value can be obtained at the same time.

2. Structural design of sensor

An integrated microfluidic metamaterial sensor with "mouth" shape is designed in this paper. The overall structure of the sensor is shown in Fig. 1 (a). The sensor consists of five layers from top to bottom, followed by a dielectric layer, a metal resonant layer (Fig. 1 (b)), a microfluidic metal plate and a dielectric substrate. The dielectric layer is made of polyethylene with relative permittivity of 2.3.The metal resonant layer and metal layer are made of gold with conductivity $\sigma = 4.52 \times 10^7 \mathrm{S/m}$ and the dielectric substrate is made of high resistivity silicon (*Si*) with relative permittivity of 11.9. The specific structural parameters of the terahertz metamaterial sensor are shown in Table 1.

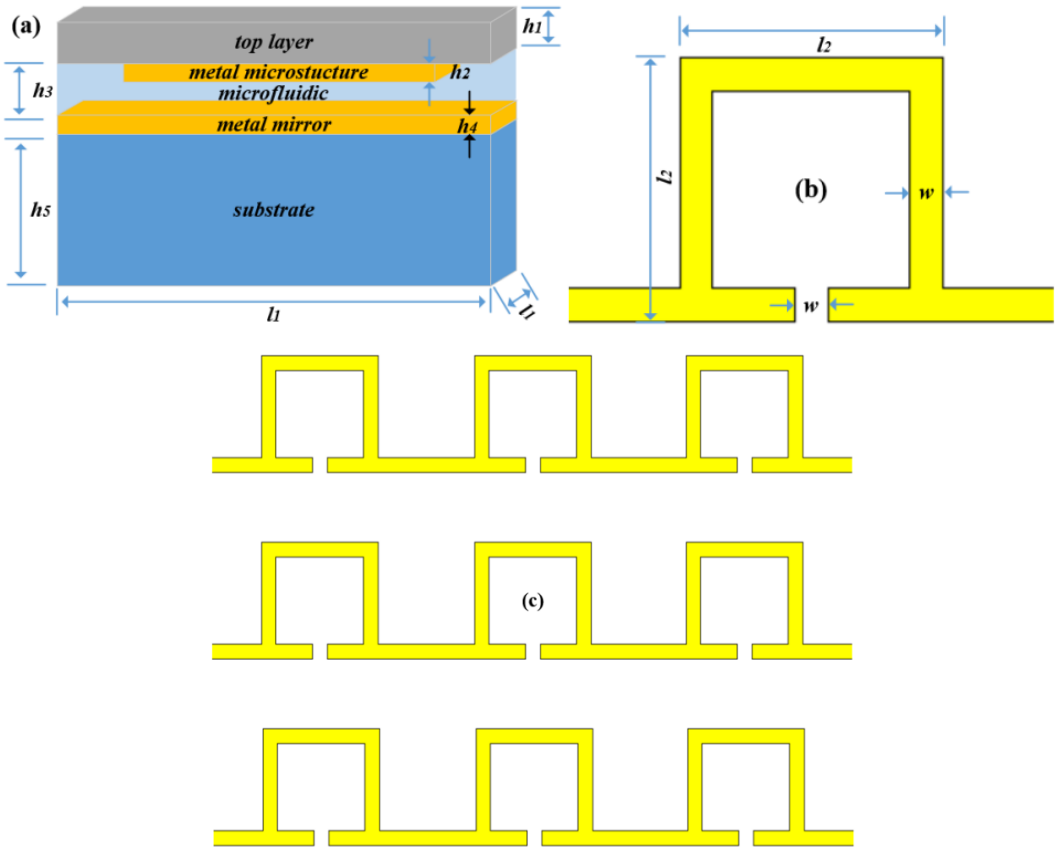

Fig. 1. THz microfluidic sensing structure diagram: (a) overall structure; (b) metal resonant structure; (c) metal resonant display (color online)

Table 1. Parameters of terahertz microfluidic biosensor

Parameters	l_1	l_2	w	h_1	h_2	h_3	h_4	h_5
Value/μm	120	100	5	4	0.1	13	0.1	50

In the design process of the sensor, in order to select the best microfluidic thickness, the terahertz time domain spectrometer (shown in Fig. 2) is used to analyze the influence of different microfluidic thickness on the performance of the sensor. Fig. 3 shows the terahertz spectrum of sensors with different microfluidic thickness.It can be seen that with the continuous increase of the height of the microfluidic, it can be seen from Fig.3 (a) that the absorptivity first increases and then decreases, and reaches 99.83% at 13 μm, which is close to perfect absorption. in addition, with the continuous increase of the thickness of the microfluidic, the *Q* value also shows a downward trend (Fig.3 (b)). When the height of the microfluidic increases from 10 μm to 20μm with a step size of 2μm, the reflectivity sensitivity of the sensor decreases from 227.8 GHz/RIU to 215.2 GHz/RIU (Fig. 3 (c)). At the same time, the *FOM* value of the sensor also shows a downward trend (Fig.3 (d)). Considering the sensitivity of the designed sensor to achieve high sensitivity, high absorptivity, high *Q* value and high *FOM* value as much as possible, the height of the microfluidic is selected as 13 μm.

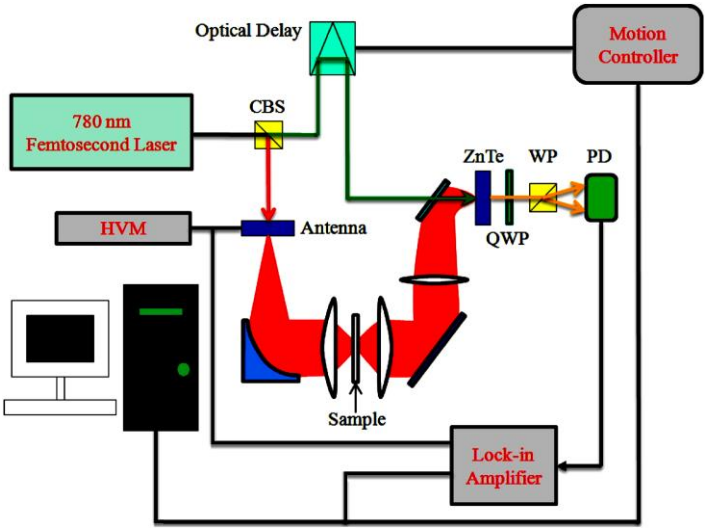

Fig. 2. Experimental setup of the THz–TDS system (color online)

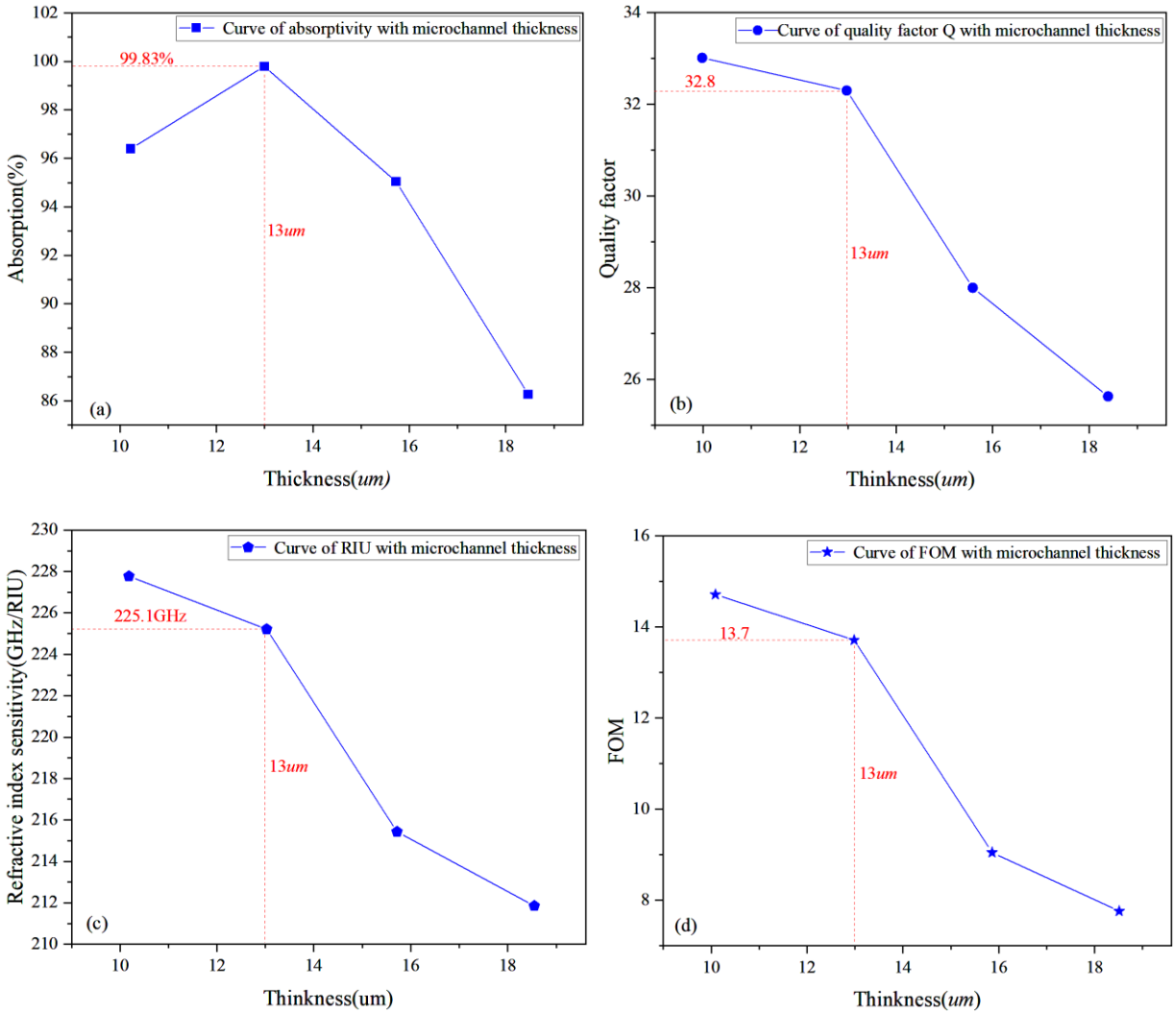

Fig. 2. Effect of microfluidic thickness on the performance of the sensor: (a) absorption; (b) quality factor; (c) refractive index sensitivity; (d) FOM (color online)

In this paper, the absorption mechanism of the metamaterial sensor is explained by the normalized effective surface impedance. Fig. 4 shows the equivalent input impedance *Z(f)* at the resonant frequency of the designed metamaterial sensor. At 0.827 THz,*Re (Z)* close to 1 THz,*Re (Z)* is close to 0. This means that the metamaterial sensor forms a good impedance match with the free space, resulting in a resonant absorption peak close to perfect absorption.

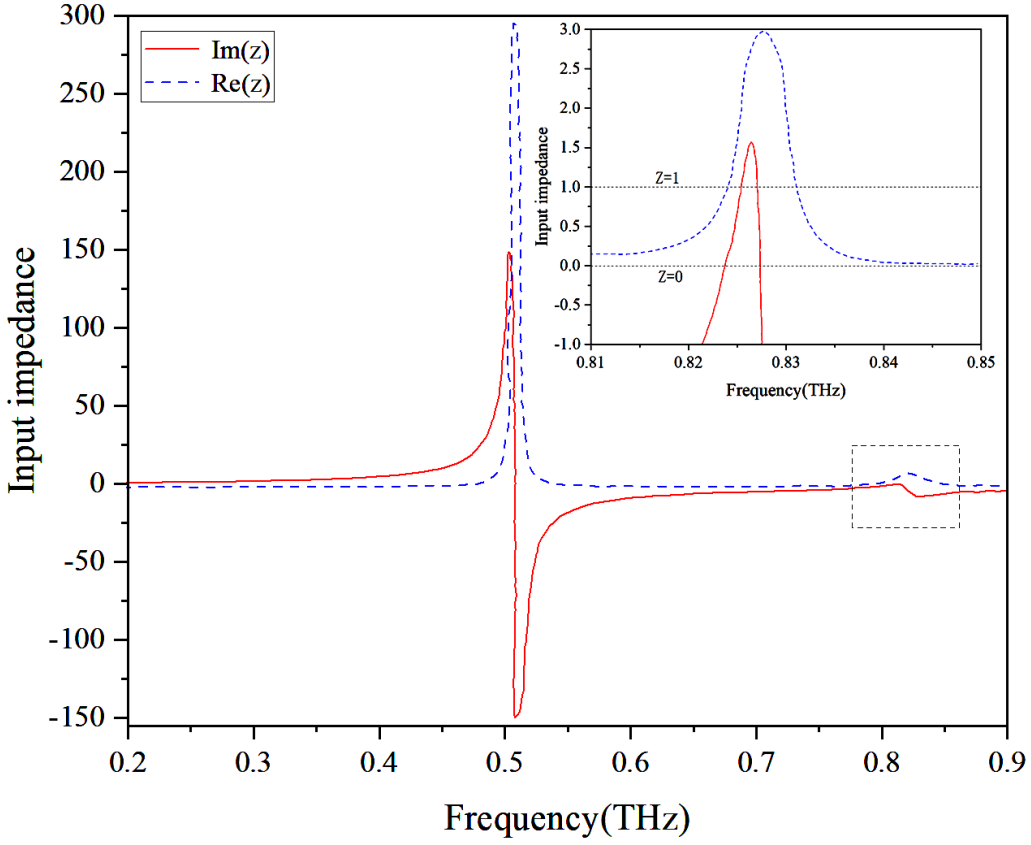

Fig. 4. Equivalent impedance real part and imaginary part of microfluidic sensor (color online)

3. Analysis of sensing performance

3.1. Sensing performance index

The quality factor *Q*: is used to characterize the optical resonance properties of the sensor. the larger the *Q* is, the smaller the loss of the resonance system is, the narrower the resonance peak is, and the easier it is to distinguish the change of the measured spectrum [22]. The *Q* of the sensor can be expressed as $Q = f_0/X_{FWHM}$. the formula, $f_0$is the resonant frequency and X_{FWHM} is the full width of the half peak.

The absorption: can be expressed as: $A(\omega) = 1 - R(\omega) - T(\omega) = 1 - |S_{11}|^2 - |S_{21}|^2$, where ω is the frequency, $R(\omega)$ is the reflectivity, $T(\omega)$ is the transmittance, S_{11} is the reflection coefficient and S_{21} is the transmission coefficient. The thickness of the metal reflector of the Hertz sensor designed in this paper is 0.1 μm, which is much larger than the skin depth of the terahertz wave in the metal. The terahertz wave can not pass through the metal reflector, and the transmittance is almost zero. that is, $T(\omega) = 0$. Reflection sensitivity *S*: is an important index to measure the performance of the sensor. the larger its value is, the easier it is to reflect the small change of dielectric properties around the sensor in the spectrum, which can be expressed as $S = \Delta f/\Delta n$.In the formula, Δf is the change of resonance frequency, Δn is the change of reflectivity, and the unit is the reflectivity unit (RIU).

The *FOM* can characterize the overall performance of the sensor and analyze the performance of the sensor

in different frequency bands more reasonably. The higher the value of *FOM* is, the better the overall performance of the sensor is. The calculation formula of *FOM* can be expressed as $X_{FOM} = S/X_{FWHM}$.

3.2. Analysis of sensing performance

In this paper, the absorption, reflection and transmission spectra of the sensor are simulated by CST microwave studio, in which there is air in the microfluidic. The simulation results are shown in Fig.5 (a). A sharp absorption peak is produced at 0.827 THz, and the absorptivity is 99.85%, which is close to perfect absorption. The full width at half maximum (FWHM) of the absorption peak is 25.21 GHz, and the quality factor Q can be calculated to be 32.8 according to $Q = f_0/X_{FWHM}$. Fig. 5 (b) shows the absorption, reflection and transmission lines of the metamaterial sensor without integrated microfluidic in the range of 0.1 to 1.5 THz. The resonant center frequency is 0.652 THz and the absorptivity is 98.16%. Compared with the sensor with integrated microfluidic, not only the resonant frequency is red-shifted, but also the absorptivity is slightly reduced, and the perfect absorption is not achieved.

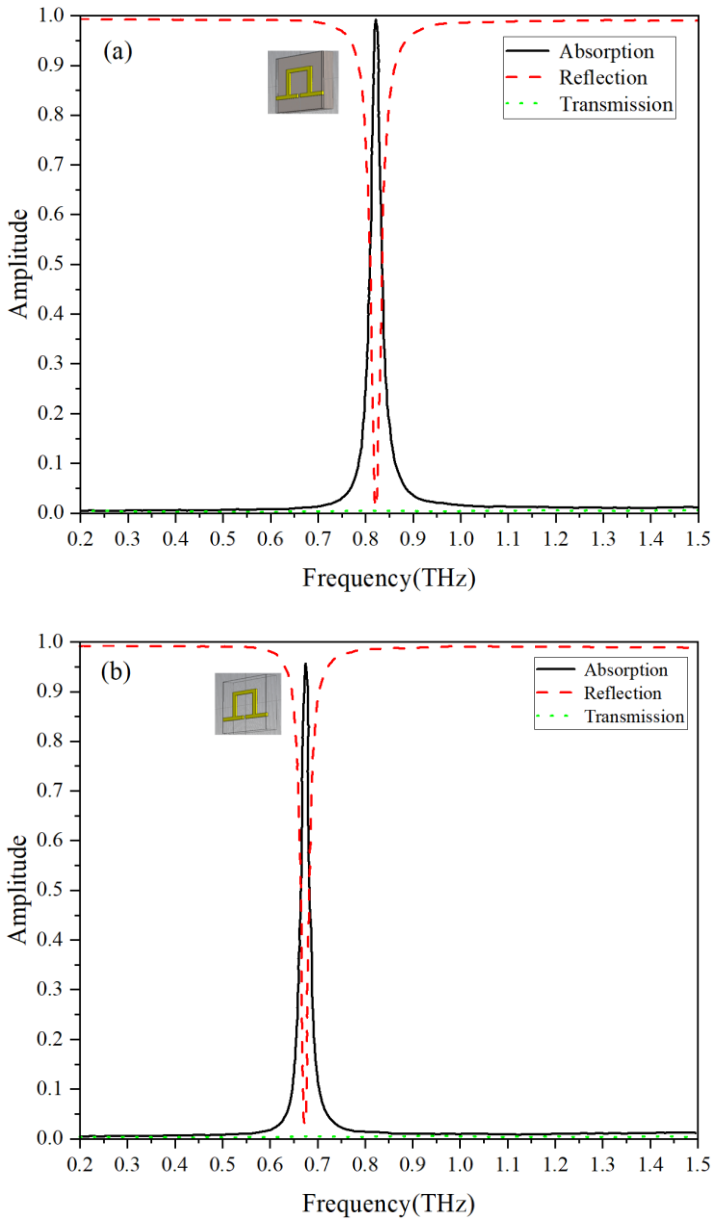

Fig. 5. Terahertz lines with or without microfluidic in metamaterial sensors: (a) absorption, reflection and transmission with microfluidic; (b) absorption, reflection and transmission without microfluidic (color online)

4. Results and discussion

In this study, the analytes with refractive index range from n=1 to n=2 are injected into the sensor with or without microfluidic, and their sensing performance is compared and analyzed. Fig.6 shows the absorption spectrum of the unintegrated microfluidic metamaterial sensor under different refractive index n of the analyte. It can be seen that the central resonant frequency corresponding to the absorption peak shows a red shift, and in the range from n=1 to n=2, the absorptivity decreases slightly with the increase of the analyte refractive index, and the absorption peak at the resonant frequency can maintain 95% absorptivity. The embedded diagram shows the trend of resonant frequency shift with the refractive index of the analyte. When the refractive index of the analyte increases gradually, the frequency offset corresponding to the resonant frequency point f increases. The linear fitting curve shows that the reflectivity sensitivity $S(f)$ at the resonant point f of the unintegrated microfluidic metamaterial sensor is 54.13 GHz/RIU, and its FOM value is about 4.1.

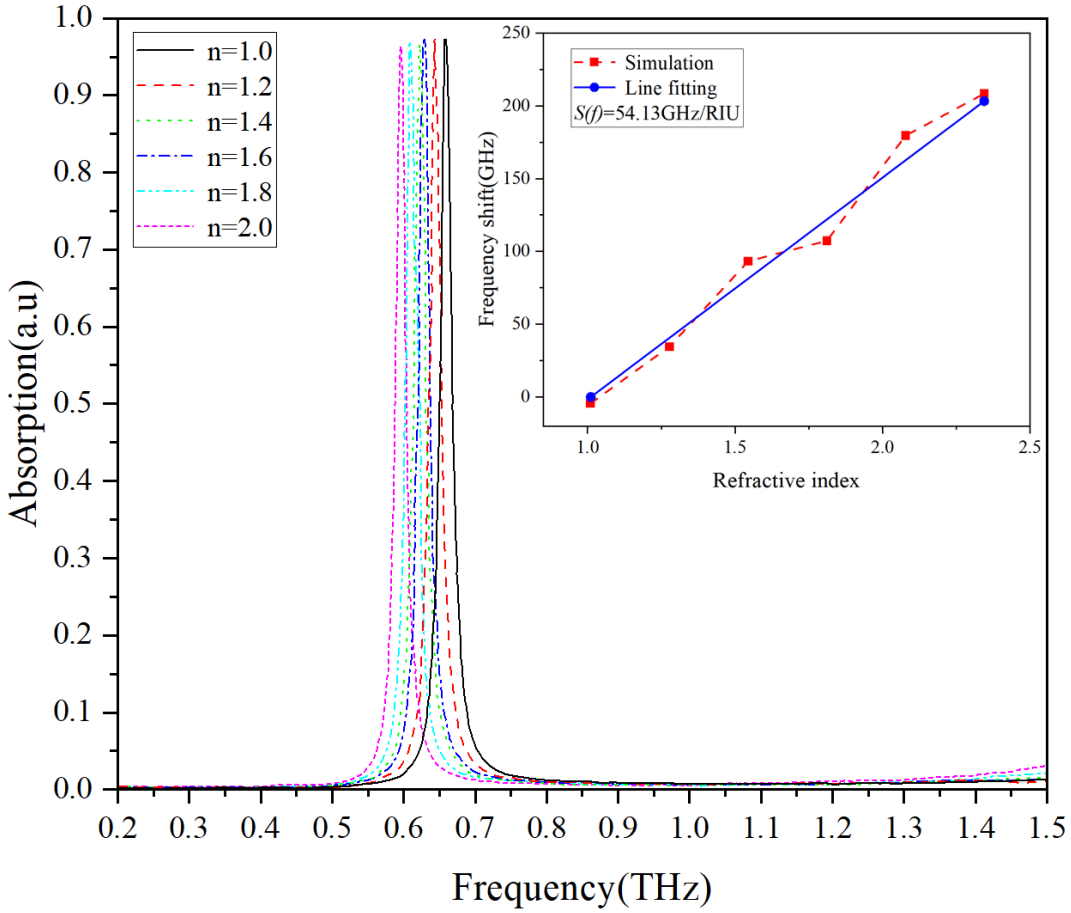

Fig. 6. Absorption spectra of metamaterial sensors (without microfluidic) under different refractive indexes. The embedded diagram shows the resonant frequency offset with different refractive index (color online)

Fig.7 shows the absorption spectrum of the integrated microfluidic metamaterial sensor under different refractive index n of the analyte. By changing the refractive index of the analyte to be measured, it can be seen that not only the central resonant frequency corresponding to the absorption peak shows a red shift, but also the absorption peak at the resonant frequency can maintain 99% absorptivity in the range from nmol 1 to nmol 1.6; when the analyte refractive index increases from nmol 1.6 to n = 2, the absorptivity of the resonant peak decreases to a certain extent, but can still be kept above 90%. The above analysis shows that the absorption peak can maintain a high absorption rate when the refractive index varies from n=1 to n=2, indicating that the sensor has good absorption stability. The embedded diagram shows the trend of resonant frequency shift with the refractive index of the analyte. When the refractive index of the analyte to be measured increases gradually, the frequency offset corresponding to the resonant frequency point f increases, and the increasing trend

gradually slows down. From the linear fitting curve, it can be known that the resonance point f of the integrated microfluidic metamaterial sensor corresponds to the reflectivity sensitivity *S(f)* = 225.1 GHz/RIU. It can be seen that the designed sensor has high sensitivity and can be used as a biosensor.

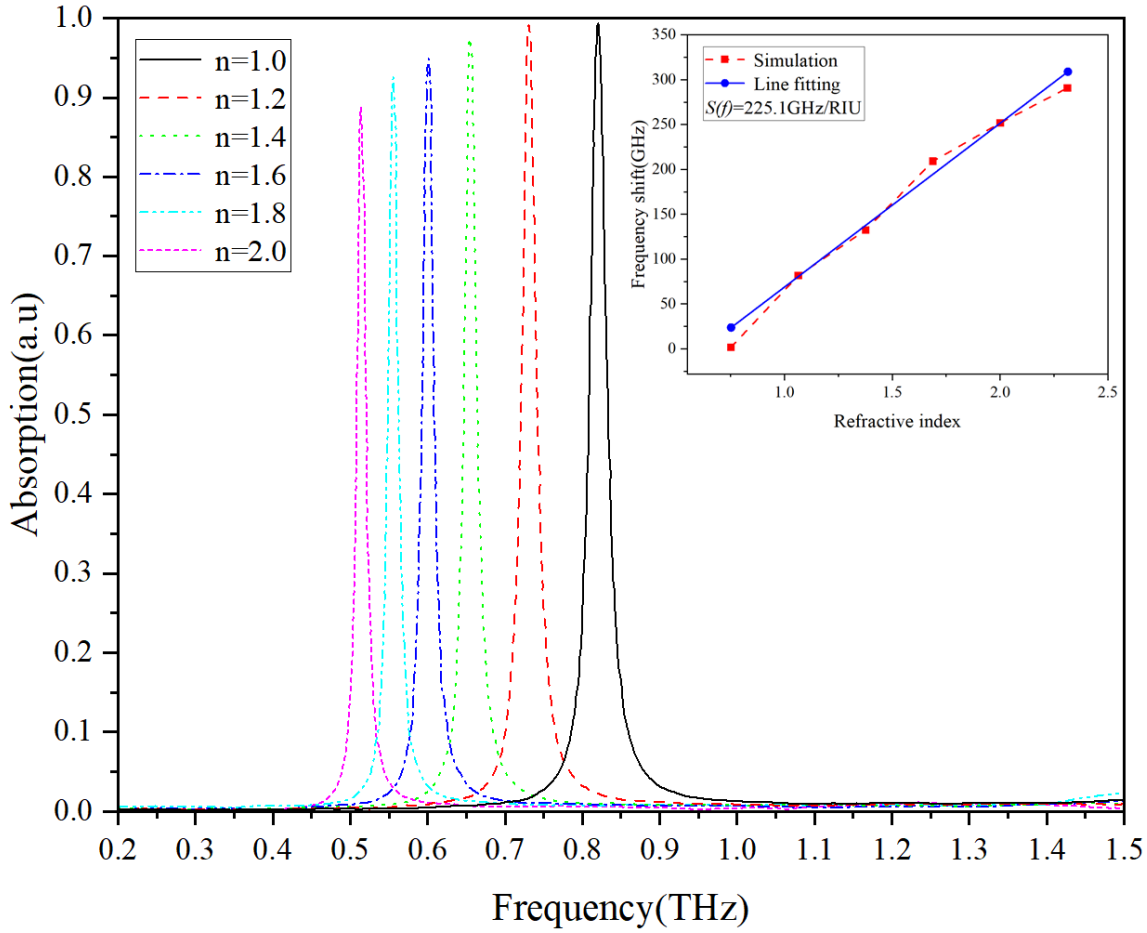

Fig. 7. Absorption spectra of metamaterial sensors (integrated microfluidic) under different refractive indices. The embedded diagram shows the resonant frequency offset with different refractive index (color online)

Table 2 shows the comparison of the performance parameters of the terahertz metamaterial sensor with and without integrated microfluidic. For the sensitivity that this study focuses on, it can be found that the refractive index sensitivity of the sensor with integrated microfluidic is about 4.1 times higher than that of the sensor without integrated microfluidic. At the same time, although the *Q* value of the sensor with integrated microfluidic is slightly smaller than that of the sensor without integrated microfluidic, it can not only achieve perfect absorption in absorptivity, but also has a higher *FOM* than the sensor without integrated microfluidic. It can be seen that the sensor integrated with microfluidic can not only greatly improve the sensitivity of the sensor, but also improve the *FOM* value of the sensor, making the performance of the sensor more excellent.

Table 2. Performance comparison of terahertz metamaterial sensors with or without integrated microfluidic

Performance parameter	Integrated microfluidic	Unintegrated microfluidic
Absorption peak frequency	0.827THz	0.625THz
Absorptivity	99.83%	98.16%
FWHM	25.21 GHz	22.81GHz
Quality factor (Q)	32.8	27.4
sensitivity (S)	225.1GHz/RIU	54.13GHz/RIU
FOM	13.7	4.1

5. Conclusions

In order to realize the direct detection of liquid samples, a single-peak metamaterial sensor with integrated microfluidic is designed in this paper. The sensor produces a near-perfect absorption peak at 0.827THz, in which the *Q* is 32.8. When the microfluidic of the sensor is injected into the analyte and the refractive index of the analyte changes from 1 to 2, the refractive index sensitivity reaches 225.1 GHz/RIU. The reflectivity sensitivity of the sensor without integrated microfluidic is 54.13 GHz/RIU. The sensitivity of the sensor with integrated microfluidic is about 4.1 times higher than that without integrated microchannel. The results show that the existence of microfluidic can not only directly detect the liquid sample, but also greatly improve the sensitivity of the sensor.

Acknowledgments

This work is supported by Natural Science Foundation of Guangdong Province(No. 2022A1515011409); supported by Key Areas Special Project of General Universities in Guangdong Province (No.2023ZDZX1024); supported in part by research grants from theYouth Project of National Natural Science Foundation of China (No.52105268); supported in part by the Key Project of Shaoguan University (No. SZ2017KJ08; SZ2020KJ02); supported in part by Youth Project of National Natural Science Foundation of China (No.62001200), supported in part by the Natural Science Foundation of Fujian Province (No.2020J01817).

References

[1] T. Zhao, P. Y. Xie, H. J. Wan, T. P. Ding, M. O. Liu, J. L. Xie, E. E. Li, X. Q. Chen, T. W. Wang, Q. Zhang, Y. Y. Wei, Y. B. Gong, Q. Y. Wen, M. Hu, C. W. Qiu, X. Xiao, Nat. Photon. **17**, 622 (2023).

[2] Y. S. Cao, Z. Cheng, R. F. Wang, X. Y. Liu, T. R. Zhang, F. Fan, Y. Huang, Carbon **199**(31), 333(2022).

[3] Yaru Wang, Lanju Liang, Maosheng Yang, Xujuan Wang, Yan Wang, Laser and Optoelectronics Progress **56**(4), 041603 (2019).

[4] J. Yang, S. Meng, Y. C. Li, Y. X. Ye, J. Tan, Q. J. Li, X. D. Ren, J. Mater. Sci.: Mater. Electron. **33**, 379 (2021).

[5] Y. Fei, X. Y. Wang, F. Wang, W. K. Xie, Q. Y. Wen, X. Xiao, Chem. Eng. J. **461**, 142049 (2023).

[6] X. Li, L. Guo, C. Gong, W. Liu, Opt. Commun. **541**, 129532 (2023).

[7] X. Q. Chen, L. Du, G. B. Jiang, Z. Wu, Y. C. Zou, Y. H. Zou, Nano Res. **16**, 10175 (2023).

[8] M. Chen, L. Singh, N. Xu, R. Singh, W. Zhang, L. Xie, Optics Express **25**(13), 14089 (2017).

[9] Jikai Xu, Zhihao Ren, Bowei Dong, Xinmiao Liu, Chenxi Wang, Yanhong Tian, Chengkuo Lee, ACS Nano **14**(9), 12159 (2020).

[10] Zhihao Ren, Yuhua Chang, Yiming Ma, Kailing Shih, Bowei Dong, Chengkuo Lee, Adv. Optical Mater. **8**(3), 1900653 (2020).

[11] Jingxuan Wei, Zhihao Ren, Chengkuo Lee, J. Appl. Phys. **128**, 240901 (2020).

[12] Yuhua Chang, Jingxuan Wei, Chengkuo Lee, Nanophotonics **9**(10), 0045 (2020).

[13] Yiming Ma, Bowei Dong, Chengkuo Lee, Nano Convergence **7**, 12 (2020).

[14] Yu-Sheng Lin, Zefeng Xu, International Journal of Optomechatronics **14**(1), 78 (2020).

[15] Jikai Xu, Yunchen Du, Chenxi Wang, International Journal of Optomechatronics **14**(1), 94 (2020).

[16] Lei Liu, Zhenguo Jiang, Syed Rahman, Md. Itrat Bin Shams, Benxin Jing, Akash Kannegulla, Li-Jing Cheng, Micromachines **7**(5), 75 (2016).

[17] Qi Tang, Min Liang, Yi Lu, Pak Kin Wong, Gerald J. Wilmink, Donna D. Zhang, Hao Xin, Sensors **16**(4), 476 (2016).

[18] S. J. Park, S. A. N. Yoon, Y. H. Ahn, RSC Advances **6**(73), 69381 (2016).

[19] Xin Hu, Gaiqi Xu, Long Wen, Huacun Wang, Yuncheng Zhao, Yaxin Zhang, David R. S. Cumming, Qin Chen, Laser and Photonics Reviews **10**(6), 962 (2016).

[20] Li Liang, Xin Hu, Long Wen, Yuhuan Zhu, Xianguang Yang, Jun Zhou, Yaxin Zhang, Ivonne Escorcia Carranza, James Grant, Chunping Jiang, David R. S. Cumming, Baojun Li, Qin Chen, Laser and Photonics Reviews **12**(11), 1800078 (2018).

[21] Zhaoxin Geng, Xiong Zhang, Zhiyuan Fan, Xiao Qing Lv, Hongda Chen, Scientific Reports **7**, 16378 (2017).

[22] Kailing Shih, Prakash Pitchappa, Lin Jin, Chia-Hung Chen, Ranjan Singh, Chengkuo Lee, Applied Physics Letters **113**(7), 071105 (2018).

_____

*Corresponding author: liujianjun@swu.edu.cn